RESEARCH PAPER

Targeting BCL-2–Dependent Neuronal Survival in Parkinson's Disease: A Drug Repurposing Study of Pioglitazone Using in Silico and Invitro Cellular Models

[1]Sudharsan Anthony Raj, [2]Santosh Mourthy, [3]Sermugapandian Nithya, [4]Sherin Silvia A and [5]Vinothini Ragothaman

[1]Department of Pharmacology, Sri Ramachandra Faculty of Pharmacy, Sri Ramachandra Institute of Higher Education and Research (DU), Chennai 600116, Tamil Nadu, India.
[2]Department of Pharmacology, Sri Ramachandra Faculty of Pharmacy, Sri Ramachandra Institute of Higher Education and Research (DU), Chennai 600116, Tamil Nadu, India.
[3]Department of Pharmacology, Sri Ramachandra Faculty of Pharmacy, Sri Ramachandra Institute of Higher Education and Research (DU), Chennai 600116, Tamil Nadu, India.
[4]Department of Pharmacology, Sri Ramachandra Faculty of Pharmacy, Sri Ramachandra Institute of Higher Education and Research (DU), Chennai 600116, Tamil Nadu, India.
[5]Department of Pharmacology, Sri Ramachandra Faculty of Pharmacy, Sri Ramachandra Institute of Higher Education and Research (DU), Chennai 600116, Tamil Nadu, India.
**Correspondence author: santoshjeevi2000@gmail.com (Santosh Mourthy)*

Received: 28th Feb, 2026; Revised: 6th March 2026; Accepted: 7th April, 2026; Available Online: 20th April, 2026

ABSTRACT
Parkinson's disease slowly destroys the brain cells responsible for producing dopamine, leaving patients with worsening movement difficulties and no treatment that can actually stop the disease from progressing. While drugs like levodopa help manage daily symptoms, they do nothing to prevent the underlying cell death. This study asked a simple but important question: could pioglitazone, a widely used diabetes medication, be repurposed to protect dying brain cells in Parkinson's disease.The research team began by mapping thousands of biological interactions using computational tools to pinpoint where pioglitazone's effects and Parkinson's disease pathways overlap. One protein kept rising to the top BCL-2, a natural cell survival switch that is notably weakened in Parkinson's patients. Computer simulations revealed that pioglitazone grips BCL-2 considerably more firmly than levodopa does, and crucially, this grip held steady throughout extended stability testing lasting 150 nanoseconds. Additional energy calculations confirmed pioglitazone binds BCL-2 more than three times as powerfully as levodopa. The drug also proved capable of crossing into the brain and satisfied all standard pharmaceutical safety benchmarks.These computational findings were then tested on living human neuronal cells deliberately damaged to replicate Parkinson's conditions. At a modest dose of just 5 µM, pioglitazone shielded roughly 71% of cells from death marginally outperforming levodopa, which achieved 64% protection but required four times the concentration.Taken together, these results make a compelling case for pioglitazone as a genuine disease-modifying candidate for Parkinson's disease, one that targets the root cause of neuronal death rather than simply easing its consequences.

Keywords: *Parkinson's disease; pioglitazone; BCL-2; drug repurposing; molecular docking; molecular dynamics; network pharmacology; neuroprotection; SH-SY5Y; PPARγ*
How to cite this article: Raj SA, Mourthy S, Nithya S, Sherin Silvia A, Ragothaman V. Targeting BCL-2–Dependent Neuronal Survival in Parkinson's Disease: A Drug Repurposing Study of Pioglitazone Using in Silico and Invitro Cellular Models. Int J Drug Deliv Technol. 2026;16(6): 396-417. DOI: 10.25258/ijddt.16.6.47
Source of support: Nil.
Conflict of interest: None

INTRODUCTION

Parkinson's Disease (PD) is a progressive neurodegenerative disorder characterized by the loss of dopaminergic neurons in the substantia nigra pars compacta, leading to debilitating motor symptoms. Despite extensive research, its etiology remains multifactorial and involving pathological processes such as alpha synuclein aggregation, mitochondrial dysfunction, oxidative stress, neuroinflammation, and apoptosis. Current treatments, most notably Levodopa, offer symptomatic relief but fail to modify disease progression. Consequently, there is an urgent and unmet need for neuroprotective or disease modifying therapies that target the underlying mechanisms of neuronal degeneration[1].

Drug repurposing finding new therapeutic uses for existing approved drugs has emerged as a promising strategy to accelerate the development of treatments for

**Author for Correspondence: santoshjeevi2000@gmail.com*

neurodegenerative diseases. This approach reduces development time, costs, and risks by leveraging established pharmacokinetic and safety profiles. Pioglitazone, a peroxisome proliferator activated receptor gamma (PPAR-γ) agonist used to treat type 2 diabetes, exhibits anti inflammatory, antioxidant, and insulin sensitizing properties[2]. Notably, epidemiological studies have reported a significantly reduced incidence of Parkinsons in diabetic patients treated with pioglitazone, suggesting potential neuroprotective effects beyond glycemic control. However, the specific molecular mechanisms through which pioglitazone may protect neurons in Parkinsons remain poorly understood a critical gap that limits its translation as a repurposed therapeutic[3].

Apoptosis, a highly regulated form of programmed cell death, plays a central role in dopaminergic neuronal loss in PD. The B-cell lymphoma 2 (Bcl-2) protein is a key anti-apoptotic regulator that maintains mitochondrial integrity and inhibits cytochrome c release and caspase activation. In both PD models and human post mortem tissue, reduced Bcl-2 expression is commonly observed, shifting the balance toward pro apoptotic signaling and neuronal demise. Building on this, we propose a novel mechanistic hypothesis, pioglitazone may confer neuroprotection, at least in part, by directly or indirectly upregulating or stabilizing Bcl-2, thereby enhancing neuronal resistance to apoptotic stimuli[4].

This thesis aims to systematically investigate this hypothesis through an integrated computational and experimental framework. First, *in silico* molecular docking and dynamics simulations will be employed to explore the potential binding interaction between pioglitazone and Bcl-2, predicting binding affinity, stability, and interaction sites. Second, these computational predictions will be validated in a physiologically relevant *in vitro* model of PD[5]. Pioglitazone was evaluated in Parkinson's cell models to study its neuroprotective effect via Bcl-2 modulation.Cells were treated with pioglitazone at different concentrations and exposed to a Parkinson's disease inducing toxin (rotenone).Cell viability was measured using the MTT assay, and cytotoxicity was assessed using the LDH assay. Overall, the study aimed to determine whether pioglitazone protects dopaminergic cells by enhancing Bcl-2–mediated survival[6].

By bridging computational prediction with functional validation in a pathomimetic cellular model, this research seeks to provide mechanistic proof of concept for pioglitazone's neuroprotective potential in Parkinsons. The findings are expected to elucidate a novel Bcl-2 mediated anti-apoptotic pathway through which pioglitazone could be repurposed, contributing a rational scientific foundation for its further evaluation as a disease modifying therapy for Parkinson's Disease[7].

MATERIALS AND METHODS

Insilico Evaluation of Pioglitazone against Parkinson's Disease:

Network Based Identification of Therapeutic Targets:
Pioglitazone was evaluated by comparing drug-associated targets with Parkinson's disease related genes using a network pharmacology approach through multiple databases[8]. **Error! Reference source not found.**depicts the flow of network interaction that illustrating the relationships between the identified genes and the disease.

SMILES Retrieval, Target Prediction, and ADME Analysis:
The compound name "Pioglitazone" was entered in the PubChem database, which is a online platform which bears a information of data of various phytoconstituents and the smiles notation of the Pioglitazone were retrieved from the data obtained through PubChem database[9]. The smiles were pasted on the website SwissTargetPrediction which is free webtool were the target can be predicted though entering smiles of the compound. The compound "Pioglitazone" targets were predicted through SwissTargetPrediction by entering smiles[10]. Through the neighbouring platform SwissADME webtool the compound Pharmacokinetics profiles such as Absorption, Distribution, Metabolism, Elimination along with the drug likeliness rules were predicted by entering the smiles of the compound Pioglitazone. The Predicted targets from Pioglitazone were further analysed through the flow of Network-interaction[11].

Gene-extraction and Intersection analysis:
The genes of the Parkinson's disease for the proposed study were retrieved through the GeneCard database which is an open-access web tool where the disease related genes can be retrieved by inputting the name of disease in search bar of the webtool[12]. The genes associated with the Parkinson's disease were extracted for the further analysis. The potential targets of Pioglitazone predicted using SwissTargetPrediction and the Parkinson's disease–associated genes obtained from GeneCards were further subjected to an intersection analysis using Venny 2.1 . Venny 2.1 is an open-access web-based tool that performs overlap analysis through Venn diagram representation. The predicted targets were entered into the first input field, while the disease-related genes were entered into the second input field. Upon executing the analysis, the common genes shared between the two datasets were identified and considered for subsequent analyses[13].

Protein–Protein Interaction Analysis for Hub Gene Discovery:
The common genes acquired from the intersection evaluation were uploaded to the STRING database for protein–protein interaction analysis, with the species selected as Homo sapiens. The interaction analysis was then performed to construct the protein–protein interaction network[14]. The PPI network image was downloaded, and the corresponding gene data were exported from the STRING database and prepared using Microsoft excel, where a filter was applied to select entries with a threshold score greater than 0.4 for subsequent analysis. The protein

interaction network obtained from the STRING database was further imported into Cytoscape software for advanced network analysis[15]. The MCC (Maximal Clique Centrality) algorithm was applied using the CytoHubba plugin to identify key nodes within the network. Based on this analysis, the top 10 hub genes that are closely associated with the disease were identified, and these genes were subsequently used for pathway visualization[16].

Identification of Significant Pathway Using KEGG Analysis:

The top 10 hub genes identified from the Cytoscape analysis were uploaded to the ShinyGO web platform to perform KEGG pathway enrichment analysis. This analysis was carried out to identify the biological pathways significantly associated with the selected hub genes. The pathways linked to these hub genes were visualized and systematically evaluated using the KEGG database. Among the identified pathways, particular attention was given to those associated with the top-ranked gene, BCL-2, due to its established relevance in neuronal survival and apoptosis. The significant pathways involving BCL-2 were further examined in the context of the molecular mechanisms underlying Parkinson's disease. This approach enabled the prediction of key signalling pathways potentially involved in disease progression and therapeutic modulation, thereby providing insight into the mechanistic functions of Pioglitazone in Parkinson's disease[17].

Gene Ontology Analysis for Biological Function Prediction:

The top 10 hubba genes were submitted to the DAVID database to perform Gene Ontology (GO) enrichment and functional annotation. This web-based platform was used to determine the biological processes, cellular components, and molecular functions associated with the predicted hub genes[18]. In the input category, "Official Gene Symbol" was chosen since the hub genes were provided in gene symbol format, and the species was set as Homo sapiens. The GO terms corresponding to each gene were then retrieved using the DAVID database. The data retrieved from the Davids database were submitted in the S.R plot for further analysis. The S.R plot is a statistical analysis and visualization platform used for data interpretation. The data's of Go enrichment terms, combined threshold scores of Biological Process (BP), Cellular Component (CC), and Molecular Function (MF) were uploaded into the S.R plot the graphical representation of Go functional categories were obtained for interpretation[19].

Structure-Based Docking of Pioglitazone with Identified Hub Targets:

To identify the binding affinity between the top 10 hub gene–encoded proteins and the test ligand Pioglitazone, molecular docking analysis was carried out using AutoDock Vina software.The active site of Pioglitazone was identified based on evidence from previously published literature. Both the protein structures and the ligand molecule were prepared according to the docking parameters required for AutoDock Vina[20]. After molecular preparation, polar hydrogens and Kollman charges were applied to the binding components. Subsequently, the grid box was set to encompass both test ligand (Pioglitazone) and target protein structures (hub gene proteins). Docking analysis was carried out individually for all 10 hub proteins with Pioglitazone[21]. Among these, the protein associated with the KEGG pathway mechanism and exhibiting a favourable binding score was selected for further evaluation. For comparative analysis, molecular docking was also performed using the standard ligand Levodopa against the selected target protein. The binding affinity of the standard ligand was then compared with that of the test ligand Pioglitazone. The docking outputs were interpreted to recognize the binding interactions and to elucidate the possible inhibitory mechanism of Pioglitazone on the selected protein target. The docked complex files of the test ligand Pioglitazone and the standard ligand Levodopa with the selected protein were subsequently used for further molecular dynamics analysis using GROMACS[22].

Dynamic Stability Analysis of Ligand–Protein Complexes:

The Crystal Structure of the protein-inhibitor complex was considered for the dynamics. The selected ligand from docking analysis BCL-2-Protein Alone [BCL-2-APO], BCL-2-Pioglitazone [BCL-2-TOP1] and BCL-2-Levodopa [BCL-2-STD] was taken. Ligand structure was selected from the antichamber. The pdb2gmx, a module of GROMACS [23], was utilized for the addition of hydrogens to the heavy atoms. First, prepared systems were vacuum reduced using the steepest descent for 1500 steps. Next, a water simple point charge (SPCE) water model was used to solvate the structures in a cubic periodic box [24],[25]. After that, the complex systems were kept at a suitable salt concentration of 0.15 M by applying the right amounts of Na and Cl counter ions. A previously published study served as the basis for the system preparation [26],[27]. Every structure that emerged from the NPT equilibration phase underwent a final production run in the NPT ensemble for 150 ns of simulation duration. Furthermore, the simulation's trajectory was examined using various tools provided by the GROMACS software package, such as the protein root mean square deviation (RMSD), root mean square fluctuation (RMSF), radius of gyration (RG), solvent accessible surface area (SASA), hydrogen bonding (H-Bond). Molecular Mechanics Poisson-Boltzmann surface area (MM-PBSA) approach was employed to understand the binding free energy BCL-2-Pioglitazone and BCL-2-Levodopa of an inhibitor with protein throughout the simulation time. A GROMACS tool g_mmpbsa was used to calculate the binding free energy. To To get a precise outcome, we evaluated BCL-2-Pioglitazone and BCL-2-Levodopa for the last 50 ns with dt 1000 frames[28].

MTT CYTOTOXICITY ASSAY

The MTT [3-(4,5-dimethylthiazol-2-yl)-2,5-diphenyltetrazolium bromide] assay is a well-established, standardised colorimetric method for determining cell

metabolic activity and viability. Active mitochondrial succinate dehydrogenase in viable cells reduces the soluble yellow MTT tetrazolium salt to insoluble purple formazan crystals. After solubilisation in DMSO, formazan is quantified spectrophotometrically at 570 nm; absorbance is directly proportional to the number of metabolically active cells. This assay is universally employed for cytotoxicity screening and CC50 determination of pharmacological agents prior to functionalcell-basedstudies.Pioglitazone[5-[[4-[2-(5-ethyl-2pyridinyl)ethoxy]phenyl]methyl]-2,4-thiazolidinedione hydrochloride] is a member of the thiazolidinedione (TZD) class of insulin sensitisers, acting as a high-affinity full agonist at the nuclear receptor peroxisome proliferator-activated receptor-gamma (PPARgamma). Beyond glycaemic control, pioglitazone has demonstrated pleiotropic neuroprotective effects including suppression of neuroinflammation (NF-kB, COX-2, iNOS), reduction of oxidative stress (Nrf2/HO-1 upregulation), attenuation of mitochondrial dysfunction, and modulation of tau phosphorylation — all highly relevant to Parkinson's disease pathology[29],[30].

SH-SY5Y human neuroblastoma cells represent one of the most widely used in vitro models for neuropharmacology research. Before conducting mechanistic experiments with pioglitazone in this model, characterisation of its acute cytotoxic profile is essential to define safe, non-toxic working concentrations. The objective of this part of the study was to determine the cytotoxic profile of pioglitazone (1–10 µM) in SH-SY5Y cells using the 24 h MTT assay, calculate the CC50 using four-parameter logistic (4-PL) non-linear regression, and identify safe concentrations for subsequent neuroprotection studies[31].

Cell Line and Culture Conditions
SH-SY5Y human neuroblastoma cells obtained from the National Centre for Cell Science (NCCS), Pune, were cultured in Dulbecco's Modified Eagle's Medium/Nutrient Mixture F-12 (DMEM/F-12, 1:1 v/v) supplemented with 10% heat inactivated fetal bovine serum (FBS), 100 U/mL penicillin, and 100 µg/mL streptomycin. Cells were maintained at 37°C in a humidified atmosphere of 5% CO2/95% air. All experiments were performed using cells in the exponential growth phase at 70–80% confluency[32].

Drug Preparation and Concentration Range
Pioglitazone hydrochloride (molecular weight: 392.9 g/mol) was dissolved in sterile dimethyl sulphoxide (DMSO) to prepare a stock solution of 10 mM, stored at −20°C. Working concentrations of 1, 2, 3, 5, 7, and 10 µM were prepared fresh by serial dilution in serum-free DMEM/F-12 immediately before use. The final DMSO concentration in all treatment wells did not exceed 0.1% (v/v), which was matched identically by the vehicle control[33].

Experimental Groups
The following experimental groups were employed:

(i) Cell Control (CC): Cells in complete medium only serves as the 100% viability reference standard.

(ii) Vehicle Control (VC): Cells treated with 0.1% DMSO confirms absence of solvent-induced cytotoxicity.

(iii) Pioglitazone Treatment Groups: Cells treated with pioglitazone at 1, 2, 3, 5, 7, and 10 µM for 24 h (n = 3 independent replicates per concentration).

MTT Assay Protocol
Cells were seeded at a density of 1×10^4 cells/well in flat-bottomed 96-well microplates and allowed to adhere for 18–24 h. Following 24 h treatment with pioglitazone at the specified concentrations, 20 µL of MTT solution (5 mg/mL in sterile PBS, filter-sterilised through 0.22 µm membrane) was added to each well. The plate was incubated for 4 h at 37°C protected from light. The medium was carefully aspirated, and 150 µL of DMSO was added per well to solubilise the purple formazan crystals with gentle orbital agitation (10 min, room temperature). Absorbance was measured at 570 nm (reference: 630 nm) using a calibrated microplate spectrophotometer[34].

Calculation of Cell Viability
Cell viability was calculated as a percentage relative to the mean cell control absorbance:

Cell Viability (%) = (OD_Treatment / OD_Cell Control Mean) × 100

Results are expressed as Mean ± Standard Deviation (SD) of three independent replicates (n = 3).

CC50 Determination by Non-Linear Regression
The CC50 was determined by fitting the percentage cell viability data against log-transformed pioglitazone concentrations using the four-parameter logistic (4-PL) sigmoid model:

V = Bottom + (Top − Bottom) / [1 + (CC50 / x)^n]

Where V = % cell viability; x = pioglitazone concentration (µM); Top = upper viability plateau (~100%); Bottom = lower plateau (~0%); CC50 = cytotoxic concentration yielding 50% cell death; n = Hill slope coefficient. Curve fitting was performed using GraphPad Prism 9.0.

Statistical Analysis
All data are expressed as Mean ± SD (n = 3 independent replicates). Statistical analysis was performed by one-way Analysis of Variance (ANOVA) followed by Dunnett's multiple comparison post-hoc test, with Bonferroni correction applied for multiple comparisons (6 drug concentrations vs vehicle control). Significance threshold: $p < 0.05$. Notation: ns = not significant ($p > 0.05$), *$p < 0.05$, **$p < 0.01$, ***$p < 0.001$, ****$p < 0.0001$. All analyses performed using GraphPad Prism 9.0 (San Diego, CA, USA).

LDH CYTOTOXICITY ASSAYS
Lactate dehydrogenase (LDH) is a cytosolic enzyme ubiquitously expressed in all nucleated cells. Under physiological conditions, LDH is retained intracellularly; however, upon loss of plasma membrane integrity associated with cell injury or death, LDH is rapidly

released into the extracellular compartment. Measurement of LDH activity in the cell culture supernatant provides a robust, quantitative, and indirect measure of cellular cytotoxicity, making the LDH assay a gold-standard complement to the MTT viability assay in pharmacological and toxicological research.

The Abbkine KTB1110 colorimetric LDH assay kit employs a coupled enzymatic reaction: released LDH catalyses the oxidation of lactate to pyruvate with concomitant reduction of NAD+ to NADH, which subsequently reduces a tetrazolium salt (INT) to a red formazan product in the presence of an electron mediator. The optical density of the formazan product, measured at 490 nm, is directly proportional to LDH activity and, hence, to the extent of cell membrane damage. Critically, this is a colorimetric method, not a fluorometric one, thereby avoiding spectral interference and photobleaching artefacts associated with fluorescence-based LDH detection.

Rotenone (5-[6H]-benzofuro[3,2-c][1]benzopyran-6-one), a naturally occurring isoflavonoid, is a potent inhibitor of mitochondrial respiratory Complex I (NADH:ubiquinone oxidoreductase). Intracellular rotenone exposure leads to electron transport chain dysfunction, excessive reactive oxygen species (ROS) generation, ATP depletion, activation of apoptotic cascades, and ultimately neuronal cell death closely recapitulating the mitochondrial dysfunction characteristic of idiopathic Parkinson's disease. The SH-SY5Y rotenone model is therefore a widely accepted in vitro Parkinson's disease paradigm.

Pioglitazone, a thiazolidinedione (TZD) PPARgamma agonist, has demonstrated pleiotropic neuroprotective properties including suppression of NF-kB driven neuroinflammation, upregulation of the Nrf2/HO-1 antioxidant pathway, preservation of mitochondrial membrane potential, and reduction of rotenone-induced ROS generation. Levodopa (L-3,4-dihydroxyphenylalanine), the current gold-standard pharmacotherapy for Parkinson's disease, serves as the appropriate pharmacological reference compound. The objective was to quantify rotenone (20 nM) induced LDH release in SH-SY5Y cells and to evaluate and compare the cytoprotective efficacy of pioglitazone (5 µM) and levodopa (20 µM) in attenuating rotenone-induced cytotoxicity[35].

B.2 Cell Culture

SH-SY5Y human neuroblastoma cells (NCCS, Pune) were cultured in DMEM/F-12 (1:1) supplemented with 10% heat-inactivated FBS, 100 U/mL penicillin, and 100 µg/mL streptomycin at 37°C with 5% CO2. Cells at 70–80% confluency in the exponential growth phase were used for all experiments.

Drug Preparation and Treatment Schedule

Rotenone was dissolved in DMSO (stock: 10 mM) and diluted to 20 nM in serum-free medium. Pioglitazone hydrochloride was dissolved in DMSO (stock: 10 mM), diluted to 5 µM. Levodopa was dissolved in sterile water (stock: 10 mM), diluted to 20 µM. All DMSO concentrations in treatment wells were ≤0.1% (v/v). Pre-treatment protocol: pioglitazone (Group 4) and levodopa (Group 5) were added to cells 2 hours before rotenone exposure to allow pharmacological conditioning. Rotenone (Groups 3–5) was then added for 24 hours. All groups were processed simultaneously[36].

Experimental Groups

Five experimental groups were employed:

(i) Group 1 : Cell Control: Cells in standard medium only. Baseline LDH reference (minimum membrane damage).

(ii) Group 2 : Vehicle Control: Cells + 0.1% DMSO. Confirms absence of solvent-induced membrane damage.

(iii) Group 3 : Disease Model (Rotenone): Cells + Rotenone (20 nM) for 24 h. Maximum cytotoxicity reference.

(iv) Group 4 : Test Drug: Pioglitazone (5 µM, 2 h pre-treatment) + Rotenone (20 nM, 24 h). Neuroprotection assessment.

(v) Group 5 : Reference Drug: Levodopa (20 µM, 2 h pre-treatment) + Rotenone (20 nM, 24 h). Positive comparator.

Abbkine KTB1110 Colorimetric LDH Assay Protocol

The LDH assay was performed using the Abbkine Intracellular LDH Assay Kit (Cat. No. KTB1110) per manufacturer's instructions. This is a colorimetric kit based on INT (2-[4-iodophenyl]-3-[4-nitrophenyl]-5-phenyl tetrazolium chloride) reduction[37].

Cells were seeded at 5×10^4 cells/well in 96-well plates and allowed to adhere for 24 h. Following treatment, culture supernatants (50 µL/well) were transferred to fresh 96-well plates on ice. 50 µL of Abbkine KTB1110 Reaction Buffer (containing lactate substrate, NAD+, electron mediator, and INT tetrazolium salt) was added to each well. Plates were incubated at 37°C for 30 minutes in the dark. Stop solution (10 µL) was added to terminate the reaction. Absorbance was measured at 490 nm (reference wavelength: 600 nm) using a microplate spectrophotometer within 5 minutes of stopping the reaction. LDH activity (U/L) was calculated from the standard curve supplied using purified LDH standards (0–500 U/L)[38].

Calculation of Cytotoxicity and Neuroprotection

The following formulae were used for quantitative assessment:

% Cytotoxicity = [(LDH_sample − LDH_control) / (LDH_rotenone − LDH_control)]

× 100

% Neuroprotection = [(LDH_rotenone − LDH_sample) / (LDH_rotenone − LDH_control)] × 100

Statistical Analysis

Data are expressed as Mean ± SD (n = 3). One-way ANOVA followed by Tukey's HSD post-hoc test was

performed. Pairwise p-values were Bonferroni-corrected (10 comparisons). Significance threshold: $p < 0.05$. Notation: ns = not significant, *p < 0.05, **p < 0.01, ***p < 0.001, ****p < 0.0001. All analyses were performed using GraphPad Prism 9.0.

RESULTS

1. Functional Classification of Pioglitazone Predicted Targets

SwissTargetPrediction mapped pioglitazone across fifteen enzyme classes, confirming its multi-target pharmacological character. Nuclear receptors were the most frequently predicted class (20%), consistent with pioglitazone's established identity as a PPAR-γ agonist. Family A G protein-coupled receptors (GPCRs), voltage-gated ion channels, and oxidoreductases each accounted for 13.3% of targets. The remaining classes kinases, cytochrome P450 enzymes, proteases, lyases, primary active transporters, and general enzymes each contributed 6.7%. This broad target spread is biologically meaningful: oxidoreductases link directly to the oxidative stress that drives mitochondrial failure in Parkinson's disease (PD), while GPCRs and kinases converge on the neuroinflammatory and survival signalling networks that are disrupted in dopaminergic neurodegeneration. Prior experimental work has confirmed that pioglitazone reduces dopaminergic neuron loss, attenuates neuroinflammation, and upregulates BCL-2 in toxin-based PD models findings that sit comfortably within this multi-class target profile.

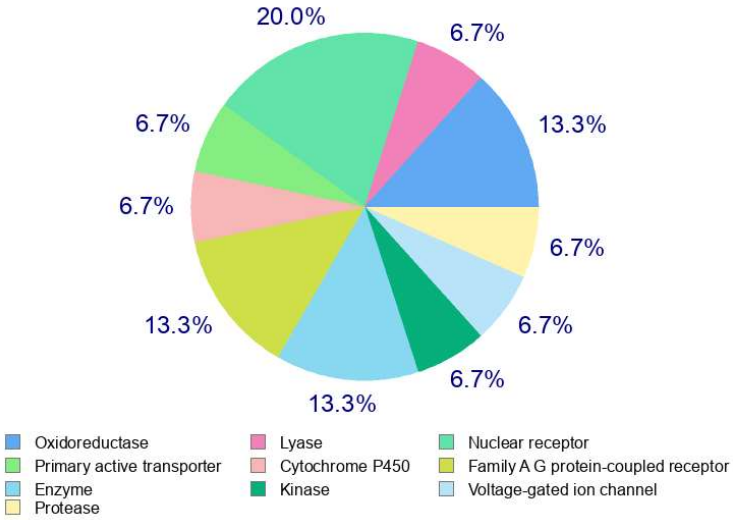

Figure 1. *Functional Enzyme Class Distribution of Pioglitazone Predicted Targets (SwissTargetPrediction).*

2. Identification of Common Genes Using Venny 2.1

Venn diagram analysis using the Venny 2.1 tool identified 77 genes (0.7%) shared between pioglitazone's predicted targets and the 10,682 PD-associated genes retrieved from GeneCards. Twenty-four genes (0.2%) were exclusive to pioglitazone, while the vast majority of PD genes (99.1%) had no overlap with the drug's predicted targets. Although the intersecting fraction appears modest, it represents a biologically meaningful set of molecular nodes through which pioglitazone could engage PD pathology. These 77 common genes were carried forward into protein-protein interaction network construction in the STRING database.

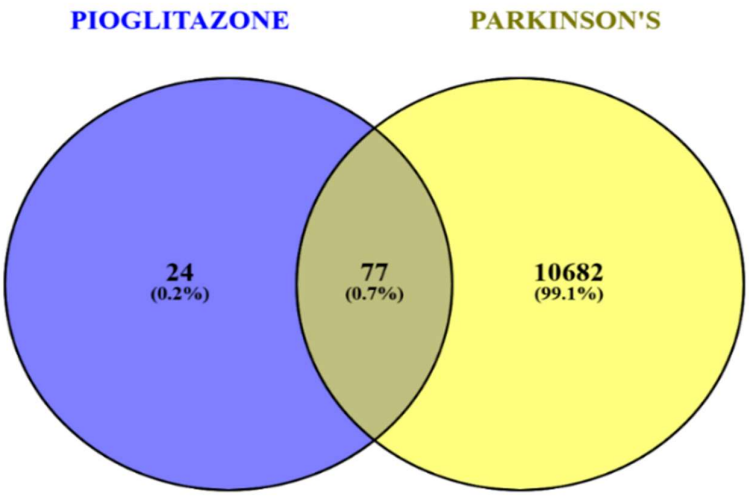

Figure 2. *Venn Diagram Showing Overlap Between Pioglitazone Predicted Targets and Parkinson's Disease-Associated Genes (Venny 2.1).*

3. Construction of the Protein–Protein Interaction Network

The 77 common genes were uploaded into the STRING database (species: Homo sapiens) to generate a protein–protein interaction (PPI) network. The resulting network revealed a dense, highly interconnected cluster of proteins, reflecting the complex molecular cross-talk relevant to both pioglitazone's pharmacology and PD pathogenesis. This systems-level representation provides a framework for pinpointing the most topologically influential proteins those acting as molecular hubs which are the most likely mediators of therapeutic effect. This approach mirrors published network pharmacology studies in PD where STRING-derived networks have successfully identified central nodes involved in neuronal survival and oxidative stress regulation.

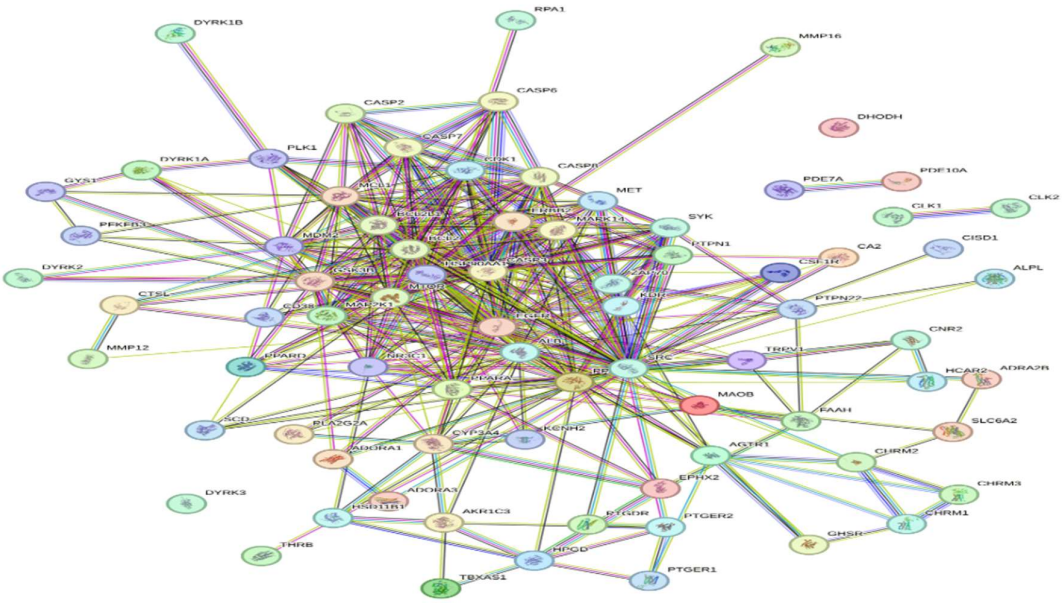

Figure 3. *Protein–Protein Interaction Network of the 77 Common Targets Constructed Using the STRING Database.*

4. CytoHubba-Based Hub Gene Identification

Topological analysis of the PPI network in Cytoscape using the CytoHubba MCC (Maximal Clique Centrality) algorithm identified the top 10 hub genes: BCL2, HSP90AA1, ERBB2, ALB, CASP8, SRC, EGFR, CASP3, MTOR, and BCL2L1. BCL2 and BCL2L1 are canonical anti-apoptotic regulators that maintain mitochondrial membrane integrity and suppress caspase-driven cell death both are downregulated in the dopaminergic neurons that die in PD. CASP3 and CASP8, the executioner and initiator caspases respectively, sit at the opposite end of the same pathway and are aberrantly activated during dopaminergic degeneration. MTOR and SRC regulate autophagy, cell survival, and neuroinflammation all

disrupted in PD while HSP90AA1 encodes a chaperone implicated in managing the alpha-synuclein aggregates that are a hallmark of PD pathology. Together, these hub genes converge on three core disease processes: apoptotic dysregulation, mitochondrial dysfunction, and impaired protein homeostasis.

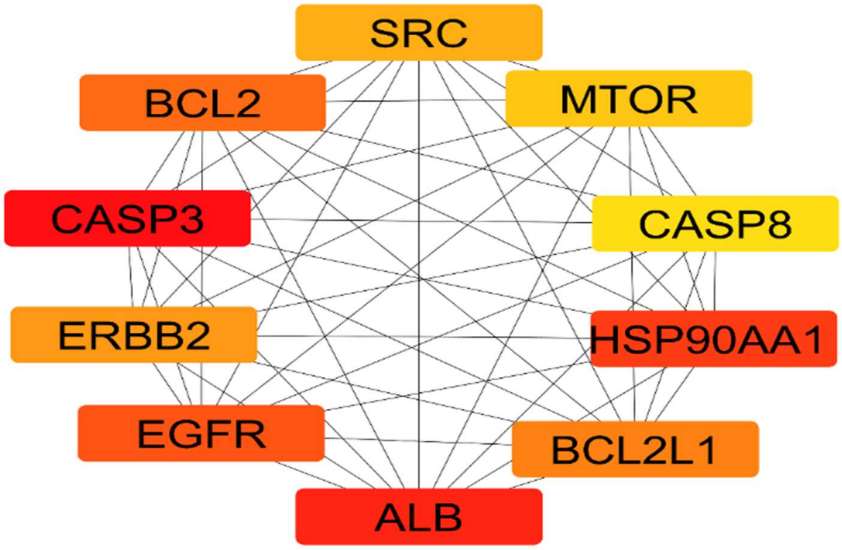

Figure 4. *Top 10 Hub Genes Identified by CytoHubba MCC Algorithm in Cytoscape from the PPI Network.*

5. Biological Pathway Annotation Using ShinyGO (KEGG)

KEGG pathway enrichment analysis via the ShinyGO platform identified the PI3K–AKT signalling pathway as the most significantly enriched route among the hub genes. This pathway integrates survival signals from growth factors and cytokines through receptor tyrosine kinases and GPCRs, ultimately activating AKT as a master pro-survival kinase. Activated AKT stimulates mTORC1-driven protein synthesis, inhibits the pro-apoptotic proteins BAD and caspase-9, suppresses GSK-3β to maintain metabolic balance, and promotes cell cycle progression. In PD, PI3K–AKT signalling is frequently under-active, contributing to apoptosis, mitochondrial dysfunction, and impaired clearance of misfolded proteins. The enrichment of this pathway among pioglitazone's hub gene targets strongly suggests that pioglitazone may restore pro-survival signalling in vulnerable dopaminergic neurons via PPAR-γ–PI3K–AKT cross-talk.

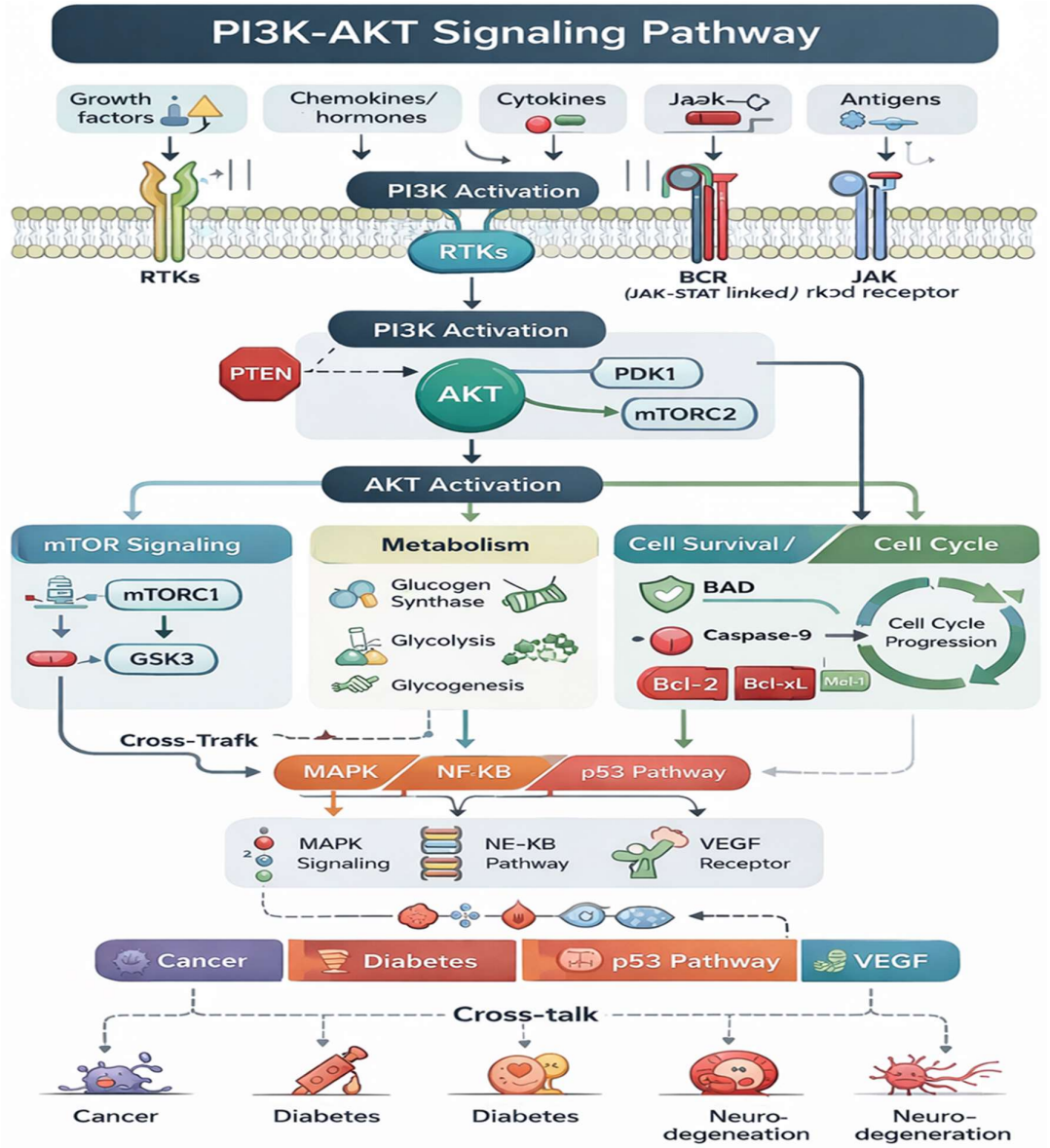

Figure 5. PI3K–AKT Signalling Pathway Enriched Among Hub Genes — Key Regulator of Neuronal Survival in Parkinson's Disease (ShinyGO/KEGG).

6. Gene Ontology (GO) Enrichment Profiling of Hub Genes

GO enrichment analysis of the top 10 hub genes was performed using the DAVID functional annotation tool and visualised with the S.R. plot. In the biological process category, the most enriched terms were regulation of apoptosis, mitochondrial depolarisation, and cell growth directly reflecting the hub genes' roles in neuronal survival and death pathways. Cellular component enrichment highlighted the mitochondrial outer membrane, cytosol, nucleus, and BCL-2 family protein complex, pinpointing the mitochondrial membrane as the primary cellular arena of action. In the molecular function category, protein binding, protein kinase activity, and ubiquitin protein ligase binding were dominant. The ubiquitin–proteasome enrichment is particularly relevant in PD, where impaired protein degradation drives alpha-synuclein accumulation and Lewy body formation. Together, the GO profile provides a coherent functional portrait of the hub genes and reinforces their collective relevance to PD pathology.

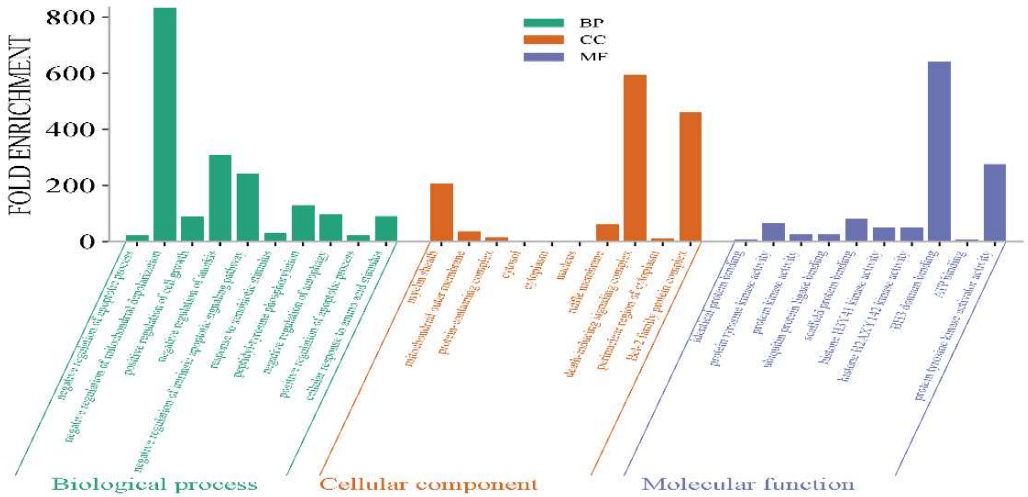

Figure 6. *Gene Ontology (GO) Enrichment Analysis of Hub Genes Across Biological Process, Cellular Component, and Molecular Function Categories (DAVID/S.R. Plot).*

7. Molecular Docking Analysis of Pioglitazone with Hub Proteins

AutoDock Vina docking of pioglitazone against all ten hub proteins yielded strongly negative binding scores across the board, indicating thermodynamically favourable interactions at each active site. Binding affinities ranged from −8.66 kcal/mol (SRC) to −16.01 kcal/mol (HSP90AA1). BCL2 was selected for in-depth comparison against the standard PD drug levodopa based on its centrality in the KEGG pathway analysis and its direct relevance to dopaminergic neuron survival. Pioglitazone bound BCL2 with an affinity of −9.42 kcal/mol, outperforming levodopa's −7.47 kcal/mol a difference of ~1.95 kcal/mol in pioglitazone's favour. The key interacting residues at the BCL2 site included TYR A:67, PHE A:63, ALA A:108, PHE A:112, VAL A:115, ARG A:105, GLY A:104, ASP A:70, GLU A:111, MET A:74, LEU A:96, and ARG A:66. The 2D and 3D interaction profiles confirmed stable, specific engagement.

Table 1: Binding Affinity Scores (kcal/mol) of Pioglitazone with Hub Proteins and Comparison with Levodopa at BCL2

S.No	Hub Protein	Ligand	Binding Score (kcal/mol)
1	BCL2	Pioglitazone	**-9.42**
2	HSP90AA1	Pioglitazone	**-16.01**
3	ERBB2	Pioglitazone	**-9.88**
4	ALB	Pioglitazone	**-8.80**
5	CASP8	Pioglitazone	**-8.91**
6	SRC	Pioglitazone	**-8.66**
7	EGFR	Pioglitazone	**-8.93**
8	CASP3	Pioglitazone	**-10.41**
9	MTOR	Pioglitazone	**-9.82**
10	BCL2L1	Pioglitazone	**-15.03**
11	BCL2	Levodopa (standard)	**-7.47**

Highlighted row = standard drug comparison. Pioglitazone shows superior BCL2 binding vs Levodopa.

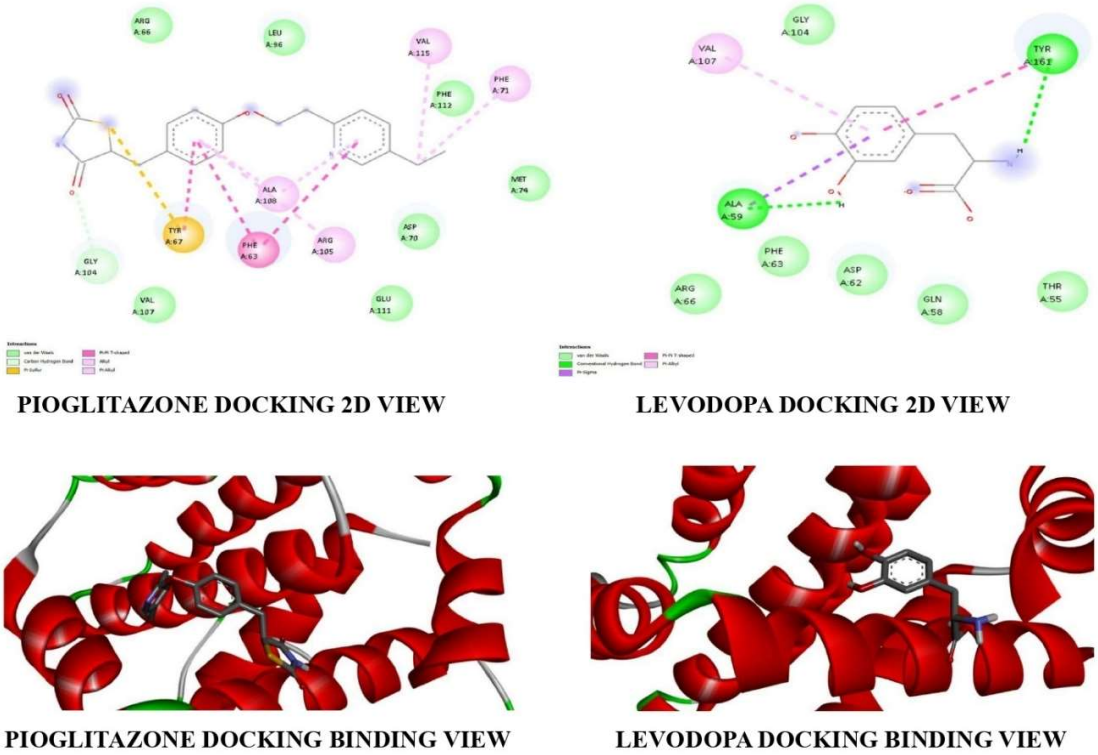

Figure 7. *2D and 3D Molecular Docking Interaction Profiles of Pioglitazone (left) and Levodopa (right) with BCL2 Protein (AutoDock Vina).*

8. Molecular Dynamics Simulation Analysis

All-atom MD simulations were conducted over 150 ns for BCL2-Pioglitazone and BCL2-Levodopa complexes, with unbound BCL2 (APO) as the reference. All three systems reached equilibrium within the first 20 ns and remained stable throughout.

Root Mean Square Deviation (RMSD)

Mean RMSD values were 0.37 ± 0.04 nm (BCL2-APO), 0.24 ± 0.04 nm (BCL2-Pioglitazone), and 0.25 ± 0.05 nm (BCL2-Levodopa). The notably lower RMSD of the pioglitazone complex compared to the free protein indicates that pioglitazone binding physically stabilises BCL2, constraining its conformational movement a hallmark of tight, specific binding.

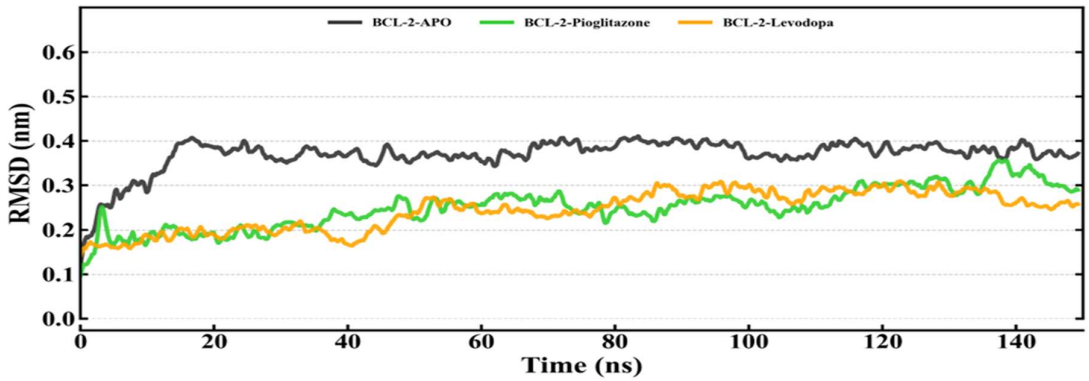

Figure 8. *RMSD Profiles of BCL2-APO, BCL2-Pioglitazone, and BCL2-Levodopa over 150 ns Simulation.*

Root Mean Square Fluctuation (RMSF)

Average RMSF values were comparable across all three systems: 0.10 ± 0.06 nm (APO), 0.10 ± 0.08 nm (Pioglitazone complex), and 0.10 ± 0.08 nm (Levodopa complex). The uniform residue-level flexibility confirms that pioglitazone engages BCL2 at a specific site without broadly perturbing the protein's dynamic behaviour consistent with selective, non-disruptive binding.

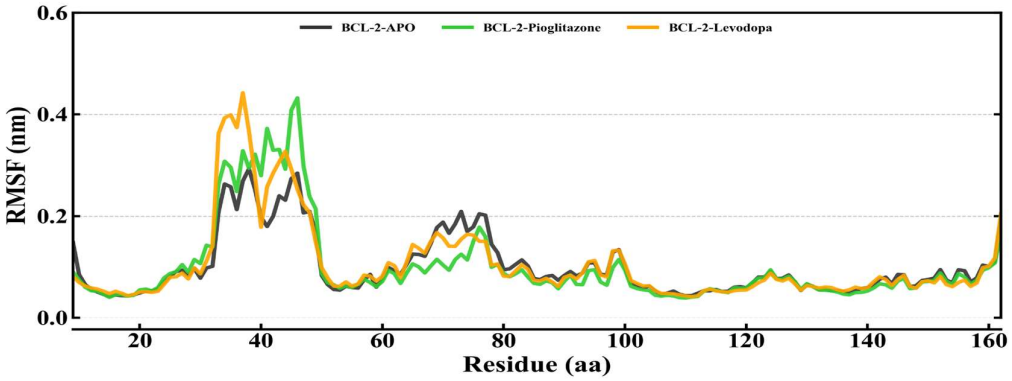

Figure 9. *RMSF Profiles of BCL2-APO, BCL2-Pioglitazone, and BCL2-Levodopa Complexes.*

Radius of Gyration (Rg)

Rg values were near-identical: 1.52 ± 0.01 nm (APO), 1.51 ± 0.01 nm (Pioglitazone), and 1.51 ± 0.01 nm (Levodopa), confirming that BCL2 maintains its native compact fold in all three systems throughout the simulation.

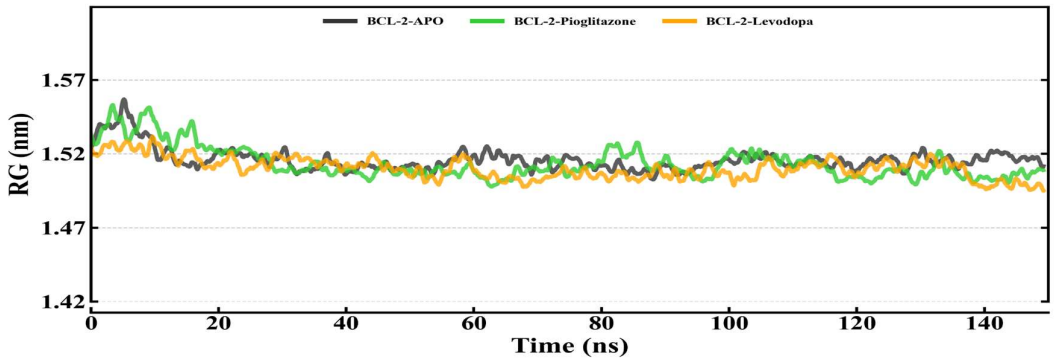

Figure 10. *Radius of Gyration (Rg) of BCL2-APO, BCL2-Pioglitazone, and BCL2-Levodopa Complexes.*

Solvent Accessible Surface Area (SASA)

Average SASA values were 85.33 ± 2.25 nm² (APO), 87.55 ± 2.27 nm² (Pioglitazone), and 88.73 ± 2.15 nm² (Levodopa). The marginal increases upon ligand binding reflect minor surface remodelling around the binding pocket, without significant disruption of the overall solvent interface.

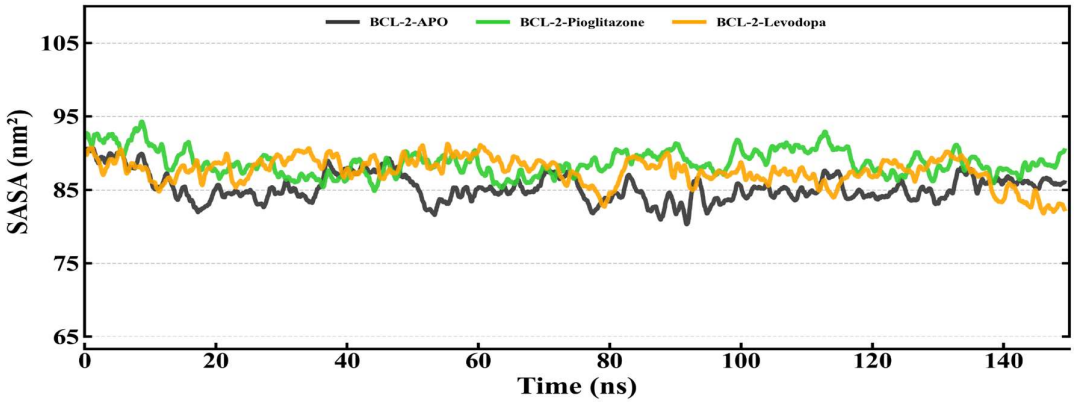

Figure 11. *SASA Profiles of BCL2-APO, BCL2-Pioglitazone, and BCL2-Levodopa Complexes.*

Hydrogen Bond Analysis

Intramolecular hydrogen bond counts were stable and comparable: 126.95 ± 6.28 (APO), 125.91 ± 6.12 (Pioglitazone), and 125.45 ± 6.35 (Levodopa), confirming preserved internal structural integrity in all systems. Intermolecular hydrogen bonds between BCL2 and each ligand ranged dynamically from 0 to 6 throughout the simulation, indicating active, sustained non-covalent interaction that contributes to complex stabilisation.

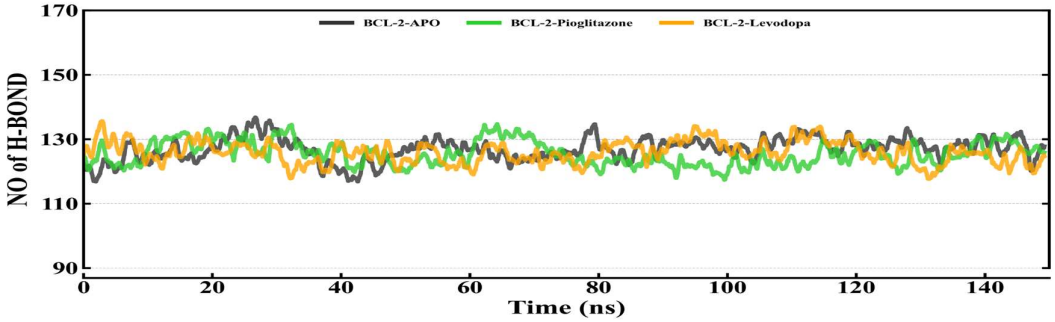

Figure 12. *Intramolecular Hydrogen Bond Counts for BCL2-APO, BCL2-Pioglitazone, and BCL2-Levodopa.*

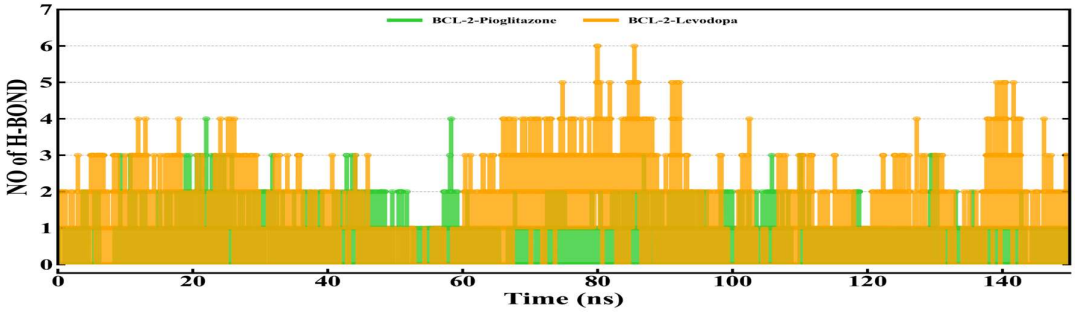

Figure 13. *Intermolecular Hydrogen Bonds Between BCL2 and Pioglitazone / Levodopa During Simulation.*

Principal Component Analysis (PCA)

PCA of conformational dynamics along the first two eigenvectors (PC1 and PC2) showed significant overlap in the conformational sampling space of all three systems. Both ligand-bound complexes displayed reduced conformational motions relative to the APO protein, indicating that pioglitazone and levodopa each constrain BCL2's dynamics without altering its fundamental structural ensemble.

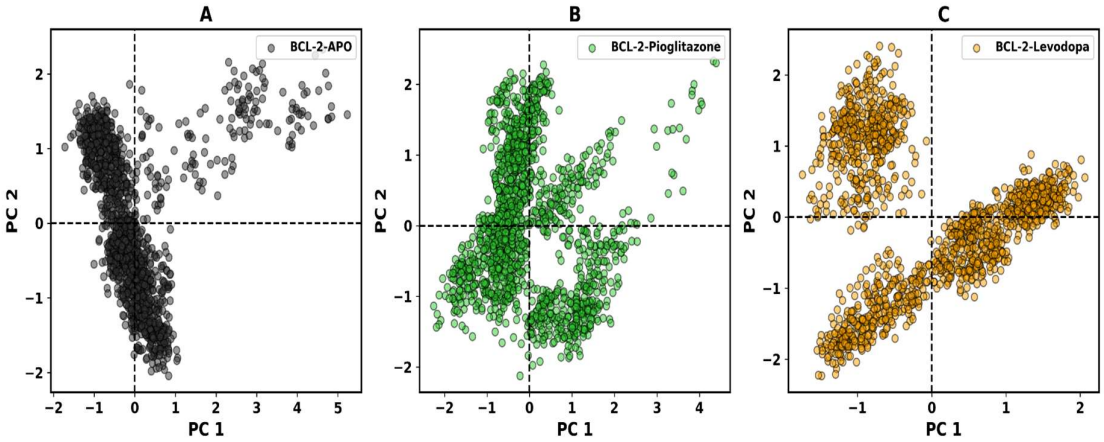

Figure 14. *PCA 2D Projection Plot Showing Conformational Sampling of BCL2-APO, BCL2-Pioglitazone, and BCL2-Levodopa on PC1 vs PC2.*

Free Energy Landscape (FEL)

FEL plots derived from PC1 and PC2 revealed a single, well-defined global energy minimum within a wide energy basin for each system (range: 0–16 kJ/mol). The single-minimum landscape for the BCL2-Pioglitazone complex confirms a thermodynamically stable, energetically favourable binding mode pioglitazone stabilises the native BCL2 conformation rather than trapping the protein in high-energy states.

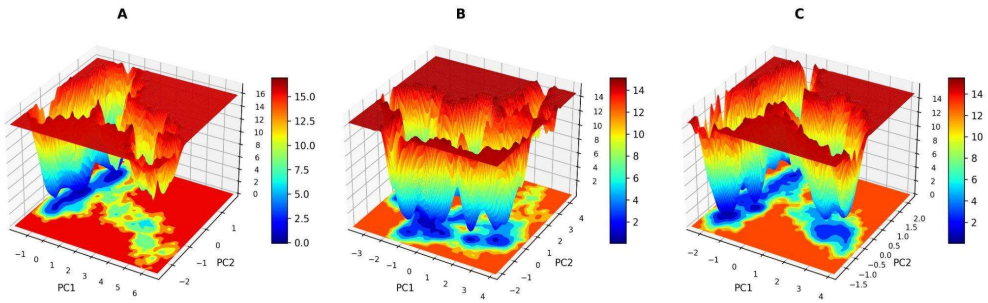

Figure 15. *Free Energy Landscape Plots for (A) BCL2-APO, (B) BCL2-Pioglitazone, and (C) BCL2-Levodopa.*

MM-PBSA Binding Free Energy Analysis

MM/PBSA binding free energy calculations provided a quantitative readout of binding strength. The BCL2-Pioglitazone complex recorded a total binding energy of −98.54 ± 12.31 kJ/mol, substantially more favourable than BCL2-Levodopa at −30.93 ± 15.65 kJ/mol — a difference of ~67.6 kJ/mol. Pioglitazone's advantage is dominated by Van der Waals interactions (−158.78 vs −74.07 kJ/mol), reflecting its larger hydrophobic surface and superior geometric complementarity within the BCL2 binding pocket. Levodopa makes proportionally stronger electrostatic contacts (−34.03 vs −18.34 kJ/mol), likely due to its ionic catechol character. Both ligands incur polar solvation penalties (desolvation costs), but pioglitazone's non-polar SASA contribution (−17.66 kJ/mol) exceeds levodopa's (−10.41 kJ/mol), further reinforcing its binding advantage.

Table 2: MM/PBSA Binding Energy Components for BCL2–Pioglitazone and BCL2–Levodopa Complexes

System	Van der Waals (kJ/mol)	Electrostatic (kJ/mol)	Polar Solvation (kJ/mol)	SASA (kJ/mol)	Total Binding (kJ/mol)
BCL2-Pioglitazone	-158.78 ± 10.58	-18.34 ± 14.31	96.24 ± 14.12	-17.66 ± 0.85	**-98.54 ± 12.31**
BCL2-Levodopa	-74.07 ± 15.61	-34.03 ± 26.70	87.58 ± 30.55	-10.41 ± 0.57	**-30.93 ± 15.65**

Green = pioglitazone; Yellow = levodopa. Pioglitazone demonstrates a ~67.6 kJ/mol stronger total binding energy, driven primarily by Van der Waals interactions.

Pharmacokinetic and Drug-Likeness Evaluation (SwissADME)

SwissADME analysis confirmed that pioglitazone possesses a pharmacokinetic profile well-suited to CNS drug repurposing. It demonstrated high gastrointestinal (GI) absorption and was predicted to be blood-brain barrier (BBB) permeable the critical prerequisite for any drug targeting dopaminergic neurons. It is not a P-glycoprotein substrate, removing a common efflux-mediated barrier to brain penetration. Pioglitazone satisfied all five major drug-likeness filters (Lipinski, Ghose, Veber, Egan, and Muegge) with zero violations and achieved a bioavailability score of 0.55. The skin permeation coefficient was −5.81 cm/s. One pharmacokinetic caution is that pioglitazone inhibits five CYP450 isoforms (CYP1A2, 2C19, 2C9, 2D6, and 3A4), which may drive drug-drug interactions in elderly PD patients on polypharmacy though this must be weighed against pioglitazone's well-characterised safety record accumulated over decades of clinical use in type 2 diabetes.

Table 3: SwissADME-Predicted Pharmacokinetic Properties and Drug-Likeness Profile of Pioglitazone

Pharmacokinetic Property	Result	Drug-Likeness Filter	Result
GI Absorption	**High**	Lipinski Rule of Five	Yes; 0 violations
BBB Permeant	**Yes**	Ghose Filter	**Yes**
P-gp Substrate	No	Veber Filter	**Yes**
CYP1A2 Inhibitor	**Yes**	Egan Filter	**Yes**
CYP2C19 Inhibitor	**Yes**	Muegge Filter	**Yes**
CYP2C9 Inhibitor	**Yes**	Bioavailability Score	0.55
CYP2D6 Inhibitor	**Yes**	—	—
CYP3A4 Inhibitor	**Yes**	—	—
Log Kp (skin)	−5.81 cm/s	—	—

Bold = favourable property. BBB permeability and zero Lipinski violations are key attributes for CNS repurposing.

MTT Cytotoxicity Assay in SH-SY5Y Cells

The cytotoxicity profile of pioglitazone was characterised across 1–10 µM in SH-SY5Y human neuroblastoma cells over 24 hours. One-way ANOVA confirmed a significant concentration-dependent effect on viability [$F(7,16) = 99.76$, $p < 0.0001$]. The vehicle control (0.1% DMSO: 99.34 ± 1.70%) was statistically indistinguishable from the cell control (100.00 ± 1.31%; $p = 1.000$), validating the experimental design. Intra-group CV% ranged from 0.6% to 3.6%, confirming excellent reproducibility. Cell viability remained ≥90% up to and including 5 µM. Statistically significant reductions first appeared at 5 µM (*$p < 0.05$), with increasing significance at 7 µM (**$p < 0.01$) and 10 µM (***$p < 0.001$). Critically, all concentrations remained above the 70% conventional cytotoxicity threshold. The extrapolated CC50 of ~25.6 µM (4-PL regression; Hill slope = 1.34) provides a >5-fold safety margin over the 5 µM pharmacological working concentration, confirming that this concentration is safe for downstream neuroprotection studies.

Table 4: Raw MTT Absorbance Values (OD at 570 nm) for Pioglitazone-Treated SH-SY5Y Cells (24 h, n = 3)

Treatment Group	Rep 1	Rep 2	Rep 3	Mean OD ± SD	CV%
Cell Control	0.8071	0.8202	0.8086	**0.8120 ± 0.0071**	0.9%
Vehicle Control (0.1% DMSO)	0.8013	0.8194	0.7992	**0.8066 ± 0.0107**	1.3%
Pioglitazone 1 µM	0.7991	0.7942	0.8120	**0.8018 ± 0.0094**	1.2%
Pioglitazone 2 µM	0.7716	0.7975	0.7904	**0.7865 ± 0.0134**	1.7%
Pioglitazone 3 µM	0.7696	0.7642	0.7733	**0.7690 ± 0.0047**	0.6%
Pioglitazone 5 µM	0.7377	0.7413	0.7134	**0.7308 ± 0.0153**	2.1%
Pioglitazone 7 µM	0.7195	0.6812	0.6731	**0.6913 ± 0.0249**	3.6%
Pioglitazone 10 µM	0.6382	0.6330	0.6287	**0.6333 ± 0.0048**	0.8%

Table 5: Percentage Cell Viability of SH-SY5Y Cells Treated with Pioglitazone (MTT Assay, 24 h, n = 3)

Group	Rep 1 (%)	Rep 2 (%)	Rep 3 (%)	Mean ± SD (%)	SEM	CV%	Sig. vs VC
Cell Control	100.21	101.19	98.60	**100.00 ± 1.31**	0.76	1.3%	—
Vehicle Control	98.05	98.70	101.27	**99.34 ± 1.70**	0.98	1.7%	**ns**
Pio 1 µM	99.46	97.91	98.85	**98.74 ± 0.78**	0.45	0.8%	**ns**
Pio 2 µM	97.70	96.32	96.56	**96.86 ± 0.74**	0.43	0.8%	**ns**
Pio 3 µM	93.85	94.99	95.28	**94.71 ± 0.76**	0.44	0.8%	**ns**
Pio 5 µM	88.33	91.39	90.29	**90.00 ± 1.55**	0.89	1.7%	*
Pio 7 µM	84.46	84.26	86.67	**85.13 ± 1.34**	0.77	1.6%	**
Pio 10 µM	77.57	77.58	78.84	**78.00 ± 0.73**	0.42	0.9%	***

**p < 0.05; **p < 0.01; ***p < 0.001 vs Vehicle Control (Dunnett's post-hoc, Bonferroni-corrected). Yellow = first significant reduction; Red = progressive cytotoxicity.*

Table 6: CC50 Determination Parameters Pioglitazone on SH-SY5Y Cells (MTT Assay, 24 h)

Parameter	Value / Interpretation
Cell line	SH-SY5Y human neuroblastoma (ATCC CRL-2266)
Test compound	Pioglitazone hydrochloride — PPARγ full agonist; TZD class
Concentration range	1, 2, 3, 5, 7, 10 µM (6 doses; 24 h)
Regression model	4-Parameter Logistic (4-PL)
CC50 (extrapolated)	~25.64 µM — >5× safety margin over 5 µM
Hill slope (n)	1.3443 — gradual, graded dose-response
Safe working dose	≤5 µM (≥90% viability maintained)

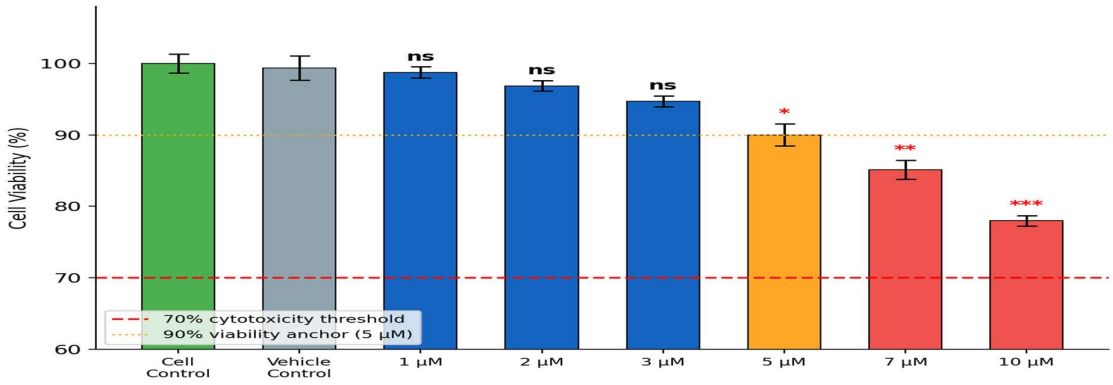

Figure 16. *Bar Graph: Percentage Cell Viability of SH-SY5Y Cells Across Pioglitazone Concentrations (MTT Assay, 24 h). Red dashed line = 70% viability threshold.*

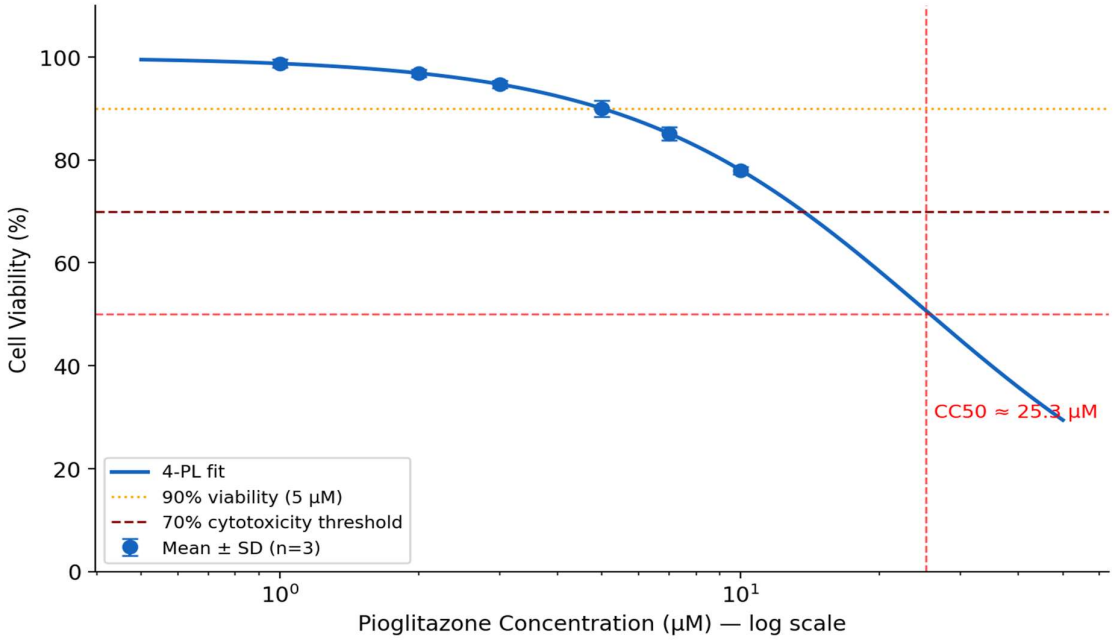

Figure 17. *4-Parameter Logistic Dose-Response Curve for Pioglitazone on SH-SY5Y Cells. CC50 ~25.6 µM (extrapolated beyond tested range).*

LDH Cytotoxicity and Neuroprotection Assay

The Abbkine KTB1110 colorimetric LDH assay was used to quantify rotenone-induced membrane damage and assess the cytoprotective efficacy of pioglitazone (5 µM) and levodopa (20 µM). One-way ANOVA confirmed a highly significant treatment effect [$F(4,10) = 895.14$, $p < 0.0001$]. Vehicle control (43.76 ± 2.99 U/L) was not significantly different from the cell control (42.18 ± 1.97 U/L; $p = 1.000$), validating solvent safety. Rotenone (20 nM) elevated LDH release approximately 3-fold to 128.54 ± 2.89 U/L, confirming robust cytotoxicity consistent with Complex I inhibition-driven mitochondrial collapse. Pioglitazone at 5 µM reduced LDH to 67.43 ± 1.88 U/L, delivering 70.76% neuroprotection ($p < 0.0001$ vs rotenone). Levodopa at 20 µM a four-fold higher molar concentration achieved 64.44% protection (72.89 ± 1.90 U/L). After Bonferroni correction for all 10 pairwise comparisons, the difference between pioglitazone and levodopa was not statistically significant ($t = -3.543$; $p_{adj} = 0.239$), confirming comparable cytoprotective efficacy. Pioglitazone therefore matches the neuroprotective benchmark of the established clinical standard at one-quarter the molar dose.

Table 7: Raw LDH Activity Values (U/L) in SH-SY5Y Cells Abbkine KTB1110 Colorimetric Assay (n = 3)

Experimental Group	Rep 1	Rep 2	Rep 3	Mean ± SD (U/L)	CV%
Cell Control (cells only)	42.49	43.98	40.07	**42.18 ± 1.97**	4.7%
Vehicle Control (0.1% DMSO)	41.50	42.63	47.15	**43.76 ± 2.99**	6.8%
Rotenone 20 nM	131.21	125.47	128.95	**128.54 ± 2.89**	2.2%
Pioglitazone 5 µM + Rotenone	69.57	66.06	66.66	**67.43 ± 1.88**	2.8%
Levodopa 20 µM + Rotenone	70.74	73.60	74.33	**72.89 ± 1.90**	2.6%

Table 8: Percentage Cytotoxicity and Neuroprotection Analysis — LDH Assay in SH-SY5Y Cells

Group	Mean ± SD (U/L)	SEM	% Cytotoxicity	% Neuroprotection	Sig. vs Rot.	Interpretation
G1: Cell Control	42.18 ± 1.97	1.14	0.00%	**100.00%**	—	Baseline
G2: Vehicle Control	43.76 ± 2.99	1.73	1.83%	**98.17%**	—	Solvent safe
G3: Rotenone 20 nM	128.54 ± 2.89	1.67	100.00%	**0.00%**	****	PD model
G4: Pioglitazone+Rot	67.43 ± 1.88	1.08	29.24%	**70.76%**	****	Strong protection
G5: Levodopa+Rot	72.89 ± 1.90	1.10	35.56%	**64.44%**	****	Comparable

Table 9: Complete Pairwise Statistical Comparisons — One-Way ANOVA with Bonferroni Post-Hoc Correction

Group A	Group B	t-stat	p (raw)	p (Bonferroni)	Sig.	Interpretation
G1	G2	-0.764	0.487	1.000	ns	No DMSO toxicity — solvent validated
G1	G3	-42.730	<0.0001	<0.0001	****	Rotenone markedly elevates LDH
G1	G4	-16.057	<0.001	<0.001	***	LDH above baseline
G1	G5	-19.430	<0.001	<0.001	***	LDH above baseline
G2	G3	-35.307	<0.0001	<0.0001	****	Rotenone vs VC confirmed
G2	G4	-11.613	<0.01	0.003	**	Pioglitazone reduces LDH
G2	G5	-14.249	<0.001	0.001	***	Levodopa reduces LDH
G3	G4	30.703	<0.0001	<0.0001	****	Pioglitazone: significant protection
G3	G5	27.872	<0.0001	<0.0001	****	Levodopa: significant protection
G4	G5	-3.543	0.024	0.239	ns	KEY: Comparable efficacy (ns after correction)

*****p < 0.0001; ***p < 0.001; **p < 0.01; ns = not significant (p > 0.05 after Bonferroni correction). Green highlighted row = primary pharmacological comparison of interest (G4 vs G5).*

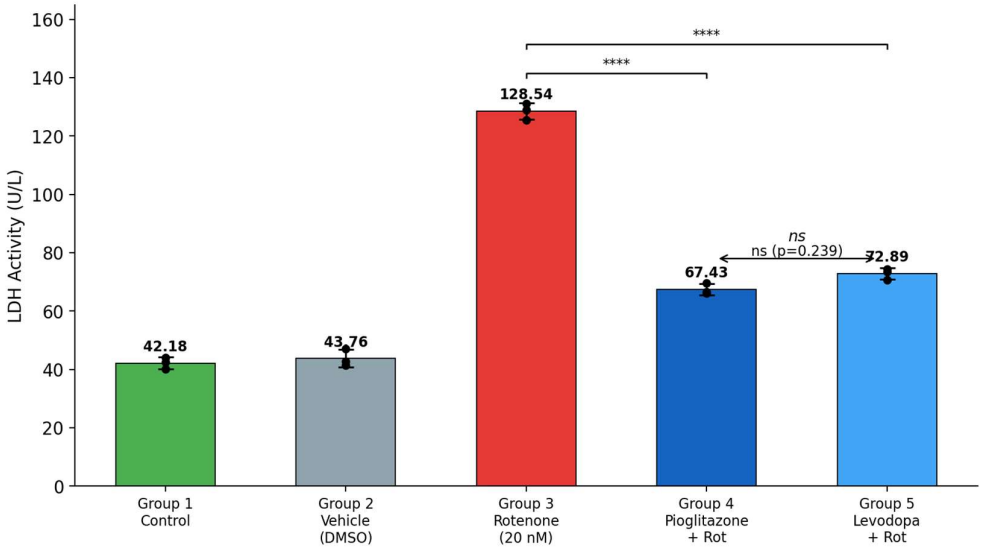

Figure 18. *LDH Activity (U/L) Across Experimental Groups — Mean ± SD (n=3). ****p < 0.0001 vs Rotenone for G4 and G5; ns between G4 and G5 (p_adj = 0.239).*

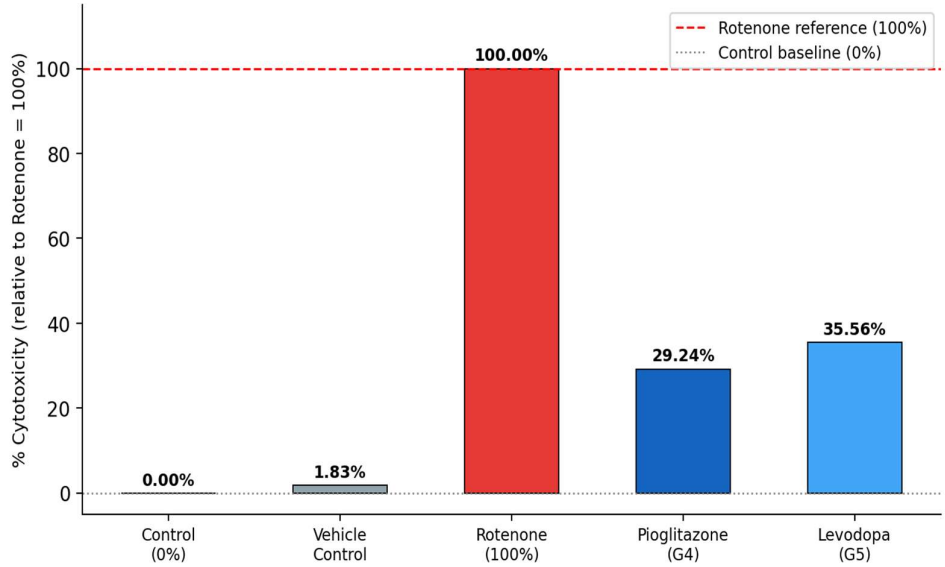

Figure 19. *Percentage Cytotoxicity Relative to Rotenone Group (= 100%; Control = 0%). Comparable values for G4 (29.24%) and G5 (35.56%) confirm equivalent protection.*

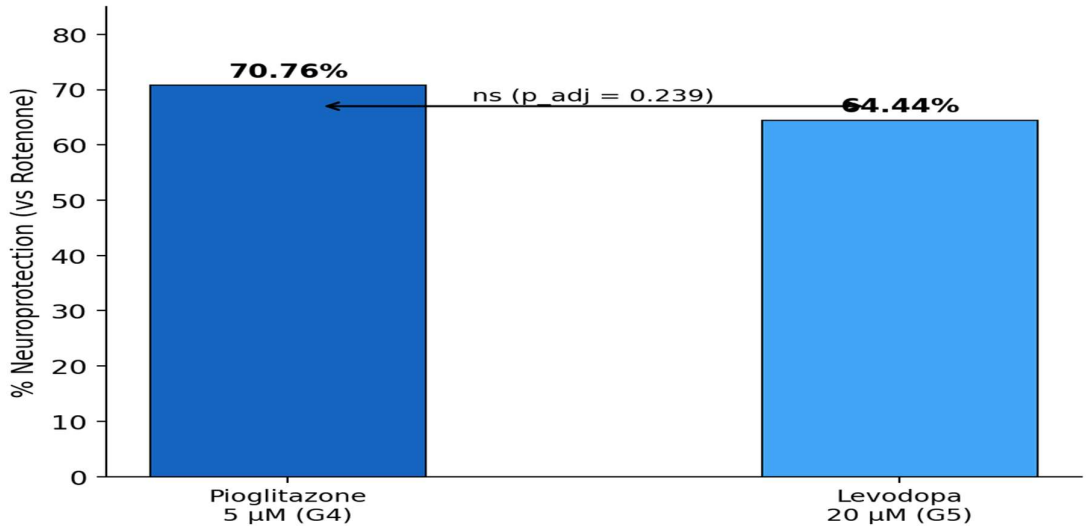

Figure 20. *Percentage Neuroprotection — Pioglitazone (70.76%) vs Levodopa (64.44%). Bidirectional 'ns' bracket confirms comparable efficacy after Bonferroni correction (t = −3.543, p_adj = 0.239).*

DISCUSSION

Pharmacological Target Landscape of Pioglitazone

Computational target prediction via SwissTargetPrediction revealed that pioglitazone acts across a surprisingly wide range of molecular targets, painting it as more than just a diabetes drug. Nuclear receptors dominated the predicted target profile (20%), which aligns perfectly with its well-known role as a PPAR-γ agonist. Activating PPAR-γ is already known to dial down inflammation and protect cells from premature death both of which are central problems in Parkinson's disease (PD). Beyond nuclear receptors, G protein-coupled receptors, voltage-gated ion channels, and oxidoreductases each accounted for 13.3% of predicted targets. The oxidoreductase hits are particularly relevant, since oxidative stress driven by mitochondrial failure is one of the earliest and most damaging events in PD. Kinases, cytochrome P450 enzymes, and proteases rounded out the profile, hinting at broad modulatory reach across intracellular signalling pathways. These computational findings resonate with experimental work showing that pioglitazone reduces dopaminergic cell loss, dampens neuroinflammation, and upregulates the survival protein BCL-2 in toxin-based PD models lending credibility to exploring it as a repurposing candidate.

Identifying the Molecular Overlap Between Pioglitazone Targets and PD Genes

Using Venny 2.1 to overlay pioglitazone's predicted targets against 10,682 PD-associated genes from GeneCards, 77 genes were found in common. While this 0.7% overlap may seem modest at first glance, it is biologically meaningful these are the very molecules where the drug and the disease intersect. This shortlist became the foundation for building a protein-protein interaction (PPI) network in the STRING database, allowing us to move from a flat gene list to a systems-level map of how these proteins talk to each other. Network pharmacology approaches like this have become a trusted route to uncovering how a single drug can influence complex disease biology, and the dense interaction cluster that emerged here sets the stage for identifying the key players worth targeting.

Hub Gene Identification and Their Relevance to Parkinson's Disease

Topological analysis of the PPI network using the CytoHubba MCC algorithm shortlisted ten hub genes: BCL2, HSP90AA1, ERBB2, ALB, CASP8, SRC, EGFR, CASP3, MTOR, and BCL2L1. Several of these are deeply tied to the very processes that go wrong in PD. BCL2 and BCL2L1 are the brain's front-line defence against mitochondrial apoptosis , they hold the outer mitochondrial membrane together, preventing the release of cytochrome c that would trigger a cell-death cascade. In contrast, CASP3 and CASP8 are the executioners of that very cascade, and both are known to be over-activated in dying dopaminergic neurons in PD. The fact that pioglitazone's network touches both the brakes and the accelerators of apoptosis is telling. MTOR and SRC govern autophagy, neuroinflammation, and cell survival all dysregulated in PD while HSP90AA1 encodes a chaperone protein that helps fold proteins correctly and has been implicated in managing the alpha-synuclein aggregates that define PD pathology. Taken together, the hub profile converges on three interconnected themes: apoptotic dysregulation, mitochondrial dysfunction, and impaired protein clearance the molecular trinity of PD.

Pathway and Gene Ontology Enrichment Analysis

KEGG pathway enrichment via ShinyGO identified the PI3K-AKT signalling pathway as the most significantly enriched route among the hub genes. This pathway acts as a cellular command centre, integrating survival signals from growth factors and cytokines to keep neurons alive. When AKT is activated, it phosphorylates a cascade of downstream targets that promote cell survival including mTOR for growth, inhibition of GSK-3β for metabolic balance, and suppression of pro-apoptotic proteins. In PD, this pathway is often underactive, contributing to neuronal

apoptosis and impaired protein clearance. The enrichment of PI3K-AKT among pioglitazone's targets suggests a plausible neuroprotective mechanism: PPAR-γ activation by pioglitazone may cross-talk with this pathway to restore its pro-survival signalling in dopaminergic neurons. Gene Ontology analysis complemented this picture elegantly. Biological process terms pointed squarely to apoptosis regulation, mitochondrial depolarisation, and cell growth. Cellular component enrichment highlighted the mitochondrial outer membrane and BCL-2 family protein complex as primary sites of action. Molecular function terms revealed protein kinase activity and ubiquitin-protein ligase binding, implicating the ubiquitin-proteasome system relevant because impaired protein clearance drives alpha-synuclein accumulation and Lewy body formation in PD. Collectively, the enrichment data provide a coherent biological narrative anchoring pioglitazone's multi-target profile to the core pathological mechanisms of PD.

Molecular Docking: Pioglitazone Outperforms Levodopa at the BCL2 Binding Site

AutoDock Vina docking against all ten hub proteins produced binding scores ranging from −8.66 kcal/mol (SRC) to −16.01 kcal/mol (HSP90AA1), with all values indicating thermodynamically favourable interactions. BCL2 was selected for in-depth analysis based on its central anti-apoptotic role and its known downregulation in PD. Pioglitazone docked to BCL2 with a binding affinity of −9.42 kcal/mol, meaningfully stronger than levodopa's −7.47 kcal/mol at the same site a difference of approximately 1.95 kcal/mol in pioglitazone's favour. The key interacting residues included TYR A:67, PHE A:63, ALA A:108, PHE A:112, VAL A:115, ARG A:105, and others lining the BCL2 hydrophobic groove. The 2D and 3D interaction profiles confirmed specific, stable engagement. The fact that pioglitazone binds BCL2 more tightly than the current gold-standard PD drug is a striking finding, suggesting it may be better positioned to stabilise or upregulate BCL2 and reinforce the cell's anti-apoptotic defences in the dopaminergic neurons most vulnerable in PD.

Molecular Dynamics Simulation and MM-PBSA Binding Energy

To move beyond the static snapshot of docking, 150-nanosecond all-atom molecular dynamics simulations were run for the BCL2-pioglitazone complex alongside BCL2-levodopa and unbound BCL2 (APO) as references. The BCL2-pioglitazone complex showed a mean RMSD of 0.24 ± 0.04 nm lower than both the BCL2-APO (0.37 ± 0.04 nm) and BCL2-levodopa (0.25 ± 0.05 nm) systems. A lower RMSD means the protein moves less when pioglitazone is bound, indicating that it physically stabilises the BCL2 structure. RMSF values were comparable across all three systems (~0.10 nm), confirming that pioglitazone binds selectively at its site rather than broadly perturbing the entire protein. Radius of gyration and SASA values were also near-identical across systems, confirming that BCL2 retains its native fold in all cases. Hydrogen bond analysis showed 0–6 intermolecular bonds between pioglitazone and BCL2 throughout the simulation, reflecting sustained non-covalent interaction. PCA revealed that both ligands constrain BCL2's conformational motions, and free energy landscape analysis identified a single, wide global energy minimum for the BCL2-pioglitazone complex a hallmark of a thermodynamically stable binding mode. MM-PBSA binding free energy calculations put the final number on the table: BCL2-pioglitazone came in at −98.54 ± 12.31 kJ/mol versus BCL2-levodopa at −30.93 ± 15.65 kJ/mol — a difference of roughly 67.6 kJ/mol. Pioglitazone's advantage is driven primarily by superior Van der Waals contacts (−158.78 vs −74.07 kJ/mol), reflecting the complementary fit of its hydrophobic surface within the BCL2 binding pocket. These simulations confirm that pioglitazone does not merely dock to BCL2 favourably on paper it maintains a stable, energetically superior interaction over physiologically relevant timescales.

Pharmacokinetic Profile and Drug-Likeness

SwissADME analysis confirmed that pioglitazone's pharmacokinetic properties are well-suited to a CNS neuroprotective role. It demonstrated high oral gastrointestinal absorption and, crucially, was predicted to be blood-brain barrier (BBB) permeable — the make-or-break requirement for any drug aiming to protect dopaminergic neurons. It is not a P-glycoprotein substrate, removing a common obstacle to brain penetration. Pioglitazone satisfied all five major drug-likeness criteria (Lipinski, Ghose, Veber, Egan, and Muegge filters) with zero violations and achieved a bioavailability score of 0.55. One clinical caveat is worth noting: pioglitazone inhibits multiple CYP450 enzymes (CYP1A2, CYP2C19, CYP2C9, CYP2D6, and CYP3A4), raising the potential for drug-drug interactions in elderly PD patients on complex medication regimens. However, this concern is balanced by pioglitazone's decades-long safety record in type 2 diabetes populations, where its tolerability is well-characterised. Overall, the ADME profile strongly supports pioglitazone's translational potential.

In Vitro Validation: MTT and LDH Assays in SH-SY5Y Cells

Computational predictions are only as good as their experimental follow-through. The MTT cytotoxicity assay in SH-SY5Y human neuroblastoma cells established that pioglitazone is well-tolerated across 1–10 µM, with all concentrations maintaining viability above 70%. At 5 µM the lowest concentration to produce a statistically significant, albeit mild, reduction (90.00 ± 1.55% viability) a CC50 of approximately 25.6 µM provides a greater than five-fold safety margin. One-way ANOVA confirmed the concentration-dependent trend [$F(7,16) = 99.76$, $p < 0.0001$], and 5 µM was selected as the safe pharmacological concentration for downstream studies. In the LDH membrane integrity assay, rotenone (20 nM) a Complex I inhibitor used to model PD's mitochondrial failure produced a robust three-fold elevation in LDH release (128.54 ± 2.89 U/L) compared to untreated cells (42.18 ± 1.97 U/L). Pioglitazone at 5 µM reduced this to 67.43 ± 1.88 U/L, corresponding to 70.76%

neuroprotection ($p < 0.0001$ vs rotenone). Levodopa at 20 µM — a four-fold higher molar concentration achieved 64.44% protection (72.89 ± 1.90 U/L). After Bonferroni correction, the difference between the two treatments was not statistically significant ($p = 0.239$), meaning pioglitazone delivers comparable protection to levodopa at a fraction of the dose. This is the study's most compelling practical finding: a metabolic drug, at a safe low concentration, matches the neuroprotective benchmark set by PD's most widely prescribed therapy. The mechanisms behind this protection likely span PPAR-γ-driven mitochondrial biogenesis, Nrf2/HO-1-mediated antioxidant response, NF-κB suppression, and direct stabilisation of mitochondrial membrane potential all converging to reduce cytochrome c release and block apoptotic cascades. Taken together, the MTT and LDH data move pioglitazone's neuroprotective potential from computational hypothesis to cell-based reality.

Integrated Interpretation

What emerges from this study is a coherent, multi-layered argument for pioglitazone as a neuroprotective repurposing candidate in PD. Network pharmacology placed BCL2 at the centre of pioglitazone's predicted mechanism. Molecular docking showed pioglitazone engages BCL2 more tightly than levodopa. Molecular dynamics confirmed that binding is stable and structurally non-disruptive over time. MM-PBSA energy calculations quantified a large thermodynamic advantage. SwissADME confirmed the drug can actually reach the brain. And in vitro experiments in a rotenone PD cell model validated the predicted neuroprotection at a safe, clinically relevant concentration. The thread running through all of this is BCL2-mediated anti-apoptotic protection a mechanism that addresses the root cause of dopaminergic neuron loss rather than simply replenishing depleted dopamine. Levodopa, for all its clinical utility, is a symptomatic treatment; pioglitazone may offer something different: a disease-modifying action that slows the death of the very cells levodopa is trying to substitute for. This study provides a strong scientific foundation for advancing pioglitazone into animal model studies and, ultimately, clinical trials focused on neuroprotection in PD.

CONCLUSION

This study investigated whether pioglitazone, a diabetes drug, can protect brain cells in Parkinson's disease by boosting a survival protein called BCL-2.Using computer based analysis, pioglitazone was found to bind strongly to the BCL-2 protein stronger than levodopa, the standard Parkinson's drug. Simulation studies confirmed that this binding was stable over time. The drug also showed good ability to reach the brain and met all the standard criteria for a safe, effective medicine.In lab experiments using human brain cells, pioglitazone successfully protected the cells from damage caused by rotenone, a toxin used to mimic Parkinson's disease. It provided about 71% protection, which was comparable to levodopa, even at a much lower dose.Overall, this study shows that pioglitazone has strong potential to be repurposed as a neuroprotective treatment for Parkinson's disease by keeping BCL-2 active and preventing brain cell death. Further studies in animals and clinical trials are needed to confirm these promising findings.

Fundings:

This research did not receive any specific grant from funding agencies in the public, commercial or not for profit sectors.

Data availability:

The authors declare that all data supporting the findings of this study are available within the article and its Supplementary Information files. Additional datasets generated or analyzed during the current study are available from the corresponding author upon reasonable request.

CRediT authorship contribution statement:

Sudharsan Anthony raj: Conceptualization, Methodology, Formal analysis, Writing – original draft. **Santosh Mourthy:** Conceptualization, Methodology, Writing – original draft, Writing – review & editing. **Dr. Nithya Sermugapandiyan:** Supervision, Conceptualization, Validation, Writing – review & editing. **Sherin Silvia A:** Data curation, Formal analysis, Writing – review & editing. **Vinothini Ragothaman:** Software, Data curation, Writing – review & editing.

Ethics Approval and Consent To Participate:

This research did not include animal subjects or human participants. All analyses were conducted using datasets and computational tools that are publicly available. Consequently, ethical approval and consent to participate were unnecessary.

Declaration of competing Interest:

The authors declare that they have no know competing financial interests or personal relationships that could have appeared to influence the work reported in this paper.

Declaration of generative AI and AI-assisted technologies in the writing process:

During the preparation of this work, the authors used ChatGPT to correct spelling, grammar, and punctuation. After using this tool/service, the authors reviewed and edited the content as needed and took full responsibility for the publication's content.

ACKNOWLEDGEMENT:

All the authors of this manuscript are thankful to their respective Departments/Universities for providing necessary facilities and support to carry out this work.

REFERENCE

1. Bhidayasiri R, Tarsy D. Treatment of Parkinson's disease: a review of pharmacological management. *Expert Rev Neurother*. 2011;11(12):1693–1712. doi:10.1586/ern.11.136.
2. Tansey MG, Wallings RL, Houser MC, Herrick MK, Keating CE, Joers V. Inflammation and immune dysfunction in Parkinson disease. *Nat Rev Immunol*. 2022;22(11):657–673. doi:10.1038/s41577-022-00684-6.

3. Kakoti BB, Bezbaruah R, Ahmed N. Therapeutic drug repositioning with special emphasis on neurodegenerative diseases: threats and issues. *Front Pharmacol*. 2022;13:1007315. doi:10.3389/fphar.2022.1007315.
4. Bernardo A, Minghetti L. PPAR-gamma agonists as regulators of microglial activation and brain inflammation. *Curr Pharm Des*. 2006;12(1):93–109. doi:10.2174/138161206780574039.
5. Feinstein DL, Spagnolo A, Akar C, Weinberg G, Murphy P, Gavrilyuk V, et al. The pioglitazone trek via human PPAR gamma: from discovery to a medicine at the FDA and beyond. *Front Pharmacol*. 2018;9:1093. doi:10.3389/fphar.2018.01093.
6. Greenamyre JT, Cannon JR, Drolet R, Mastroberardino PG. Lessons from the rotenone model of Parkinson's disease. *Trends Pharmacol Sci*. 2010;31(4):141–142. doi:10.1016/j.tips.2009.12.006.
7. Youle RJ, Strasser A. The BCL-2 protein family: opposing activities that mediate cell death. *Nat Rev Mol Cell Biol*. 2008;9(1):47–59. doi:10.1038/nrm2308.
8. Zhang Z, Li B, Huang J, Huang S, He D, Peng W, Zhang S. A Network Pharmacology Analysis of the Active Components of the Traditional Chinese Medicine Zuojinwan in Patients with Gastric Cancer. Med Sci Monit. 2020;26:e923327.
9. Kim S, Chen J, Cheng T, Gindulyte A, He J, He S, et al. PubChem 2019 update: improved access to chemical data. Nucleic Acids Res. 2019;47:D1102–9.
10. Daina A, Michielin O, Zoete V. SwissTargetPrediction: updated data and new features for efficient prediction of protein targets of small molecules. Nucleic Acids Res. 2019;47:W357–64.
11. Daina A, Michielin O, Zoete V. SwissADME: a free web tool to evaluate pharmacokinetics, drug-likeness and medicinal chemistry friendliness of small molecules. Sci Rep. 2017;7:42717.
12. Stelzer G, Rosen N, Plaschkes I, Zimmerman S, Twik M, Fishilevich S, et al. The GeneCards Suite: From Gene Data Mining to Disease Genome Sequence Analyses. Curr Protoc Bioinformatics. 2016;54.
13. Lam F, Lalansingh CM, Babaran HE, Wang Z, Prokopec SD, Fox NS, et al. VennDiagramWeb: a web application for the generation of highly customizable Venn and Euler diagrams. BMC Bioinformatics. 2016;17:401.
14. Szklarczyk D, Gable AL, Lyon D, Junge A, Wyder S, Huerta-Cepas J, et al. STRING v11: protein–protein association networks with increased coverage, supporting functional discovery in genome-wide experimental datasets. Nucleic Acids Res. 2019;47:D607–13.
15. Shannon P, Markiel A, Ozier O, Baliga NS, Wang JT, Ramage D, et al. Cytoscape: A Software Environment for Integrated Models of Biomolecular Interaction Networks. Genome Res. 2003;13:2498–504.
16. Chin C-H, Chen S-H, Wu H-H, Ho C-W, Ko M-T, Lin C-Y. cytoHubba: identifying hub objects and sub-networks from complex interactome. BMC Syst Biol. 2014;8:S11.
17. Ge SX, Jung D, Yao R. ShinyGO: a graphical gene-set enrichment tool for animals and plants. Bioinformatics. 2020;36:2628–9.
18. Huang DW, Sherman BT, Lempicki RA. Systematic and integrative analysis of large gene lists using DAVID bioinformatics resources. Nat Protoc. 2009;4:44–57.
19. Tang D, Chen M, Huang X, Zhang G, Zeng L, Zhang G, et al. SRplot: A free online platform for data visualization and graphing. PLoS One. 2023;18:e0294236.
20. Trott O, Olson AJ. AutoDock Vina: Improving the speed and accuracy of docking with a new scoring function, efficient optimization, and multithreading. J Comput Chem. 2010;31:455–61.
21. Satpute UM, Rohane SH. Efficiency of AUTODOCK: Insilico study of Pharmaceutical Drug Molecules. Asian J Res Chem. 2021;14:1–5.
22. Buckley ME, Ndukwe ARN, Nair PC, Rana S, Fairfull-Smith KE, Gandhi NS. Comparative Assessment of Docking Programs for Docking and Virtual Screening of Ribosomal Oxazolidinone Antibacterial Agents. Antibiotics. 2023;12:463.
23. Malekipour MH, Shirani F, Moradi S, Taherkhani A. Cinnamic acid derivatives as potential matrix metalloproteinase-9 inhibitors: molecular docking and dynamics simulations. Genomics Inform. 2023;21:e9.
24. Malik A, Kohli M, Jacob NA, Kayal A, Raj TK, Kulkarni N, et al. In silico screening of phytochemical compounds and FDA drugs as potential inhibitors for NSP16/10 5' methyl transferase activity. J Biomol Struct Dyn. 2023;41:221–33.
25. Satapathy P, Prakash JK, Gowda VC, More SS, K M, Chandramohan V, et al. Targeting Imd pathway receptor in Drosophila melanogaster and repurposing of phyto-inhibitors: structural modulation and molecular dynamics. J Biomol Struct Dyn. 2022;40:1659–70.
26. Kumar B, Parasuraman P, Murthy TPK, Murahari M, Chandramohan V. In silico screening of therapeutic potentials from Strychnos nux-vomica against the

dimeric main protease (Mpro) structure of SARS-CoV-2. J Biomol Struct Dyn. 2022;40:7796–814.

27. Gangadharappa BS, Sharath R, Revanasiddappa PD, Chandramohan V, Balasubramaniam M, Vardhineni TP. Structural insights of metallo-beta-lactamase revealed an effective way of inhibition of enzyme by natural inhibitors. J Biomol Struct Dyn. 2020;38:3757–71.
28. Genheden S, Ryde U. The MM/PBSA and MM/GBSA methods to estimate ligand-binding affinities. Expert Opin Drug Discov. 2015;10:449–61.
29. Mosmann TR. Rapid colorimetric assay for cellular growth and survival: application to proliferation and cytotoxicity assays. J Immunol Methods. 1983;65(1):55–63.
30. Kumar P, Nagarajan A, Uchil PD. Analysis of Cell Viability by the Lactate Dehydrogenase Assay. Cold Spring Harb Protoc. 2018;2018(6). doi:10.1101/pdb.prot095497.
31. Kovalevich J, Langford D. Considerations for the Use of SH-SY5Y Neuroblastoma Cells in Neurobiology. In: Neuronal Cell Culture: Methods and Protocols. Methods Mol Biol. 2013;1078:9–21.
32. Biedler JL, Roffler-Tarlov S, Schachner M, Freedman LS. Multiple neurotransmitter synthesis by human neuroblastoma cell lines and clones. Cancer Res. 1978;38(11 Pt 1):3751–7.
33. Betarbet R, Sherer TB, MacKenzie G, Garcia-Osuna M, Panov AV, Greenamyre JT. Chronic systemic pesticide exposure reproduces features of Parkinson's disease. Nat Neurosci. 2000;3(12):1301–6.
34. Sherer TB, Betarbet R, Testa CM, Seo BB, Richardson JR, Kim JH, et al. Mechanism of toxicity in rotenone models of Parkinson's disease. J Neurosci. 2003;23(34):10756–64.
35. Dehmer T, Heneka MT, Sastre M, Dichgans J, Schulz JB. Protection by pioglitazone in the MPTP model of Parkinson's disease correlates with IκBα induction and block of NFκB and iNOS activation. J Neurochem. 2004;88(2):494–501.
36. Barbiero JK, Santiago RM, Persike DS, da Silva Fernandes MJ, Tonin FS, da Cunha C, et al. Neuroprotective effects of peroxisome proliferator-activated receptor alpha and gamma agonists in model of parkinsonism induced by intranigral injection of LPS in rats. Neurotox Res. 2014;25(1):51–62.